−900 Å and wüstite thicknesses are 100 and 115 Å. The model used here is an ordered one with all vacancies placed in the same locations for the whole of the crystal. One can see figures similar to those obtained on the [110] projection by Ishiguro & Nagakura (1985, 1986).

IV. Discussion and concluding remarks

For the images obtained with an electron beam parallel to the [100] axis, there is no doubt that the images computed with the (10/4) cluster model fit the experimental image obtained by Ishiguro & Nagakura (1985, 1986) much better than the images computed by them with a (6/0) or (6/2) cluster model. We can even explain the variation of contrast observed in the image by a slight change in the wüstite flake thickness.

When the electron beam is parallel to the [110] axis, a difference appears between our computed images and the experimental HREM image. However, this is easily explained by the existence of some disorder concerning the stacking of the negative and positive clusters (remember that one cluster is obtained from the other by a 90° rotation about the [100] axis) because there is no reason why there should only be positive clusters stacked on top of each other. In addition, stacking faults can be clearly observed in the [100] direct images of Ishiguro & Nagakura (1985, 1986). If one postulates the existence of disorder in the stacking, the rhombs remain rhombs, but the dense lines become centered rectangles, in which case the experimental HREM images are quite well fitted.

In this study, we have shown that simulated images of the defect structure of quenched wüstite P'', based on layers of (10/4) clusters, is consistent with the observed HREM direct images obtained by Ishiguro & Nagakura (1985, 1986) and Iijima (1974). This consistency leads to an understanding of a great number of converging structural observations found in the literature, especially the value of the ratio $R = (z + t)/t = 2{\cdot}4$ found in a new set of neutron diffraction experiments (Gavarri, Jasienska, Orewczyk & Janowski, 1987; Carel & Gavarri, 1990).

References

ANDERSSON, A. B., GRIMES, R. W. & HEUER, A. H. (1984). *J. Solid State Chem.* **55**, 353–361.

ANDERSSON, A. B. & SLETNES, J. O. (1977). *Acta Cryst.* A**33**, 268–276.

CAREL, C. & GAVARRI, J.-R. (1990). *J. Phys. Chem. Solids*, **51**, 1131–1136.

CATLOW, C. R. A. & FENDER, B. E. F. (1975). *J. Phys. C*, **8**, 3267–3279.

CHEETHAM, A. K., FENDER, B. E. F. & TAYLOR, R. I. (1971). *J. Phys. C*, **4**, 2160–2165.

COWLEY, J. M. (1975). *Diffraction Physics*. Amsterdam: North Holland.

GARTSTEIN, E. Z., MASON, T. O. & COHEN, J. B. (1986). *J. Phys. Chem. Solids*, **47**, 759–773, 775–781.

GAVARRI, J.-R. & CAREL, C. (1989). *Phase Transit.* **14**, 103–108.

GAVARRI, J.-R., CAREL, C., JASIENSKA, ST. & JANOWSKI, J. (1981). *Rev. Chim. Miner.* **18**, 608–624.

GAVARRI, J.-R., CAREL, C. & WEIGEL, D. (1979). *J. Solid State Chem.* **29**, 81–95.

GAVARRI, J.-R., CAREL, C. & WEIGEL, D. (1988). *C. R. Acad. Sci.* **307**(II), 705–711.

GAVARRI, J.-R., JASIENSKA, ST., OREWCZYK, J. & JANOWSKI, J. (1987). *Metal. Odlew. Krakow*, **13**, 1–2, 43–62.

IIJIMA, S. (1974). *Electron Microsc. Soc. Am.* **32**, 352–353.

ISHIGURO, T. & NAGAKURA, S. (1985). *Jpn. J. Appl. Phys.* **24**, L723–L726.

ISHIGURO, T. & NAGAKURA, S. (1986). Proc. XIth Int. Congr. Electron Microsc., Kyoto, pp. 963–964.

KOCH, F. B. & COHEN, J. B. (1969). *Acta Cryst.* B**25**, 275–287.

LEBRETON, C. & HOBBS, L. W. (1983). *Radiat. Eff.* **74**, 227–236.

VALLET, P. & CAREL, C. (1989). *Bull. Alloy Phase Diagrams*, **10**, 209–218.

Acta Cryst. (1991). B**47**, 337–344

Structures and Phase Transitions of $[(CH_3)_4As]_2CoCl_4$ and $[(CH_3)_4As]_2ZnCl_4$

BY F. J. ZÚÑIGA, M. J. CABEZUDO AND G. MADARIAGA

Departamento de Física de la Materia Condensada, Facultad de Ciencias, Universidad del País Vasco, Apdo 644, *Bilbao, Spain*

AND M. R. PRESSPRICH, M. R. BOND AND R. D. WILLETT

Department of Chemistry, Washington State University, Pullman, Washington 99165, *USA*

(*Received* 9 *July* 1990; *accepted* 26 *November* 1990)

Abstract

Two phase transitions of bis(tetramethylarsonium) tetrachlorocobaltate(II), $[(CH_3)_4As]_2CoCl_4$, and bis(tetramethylarsonium) tetrachlorozincate(II), $[(CH_3)_4As]_2ZnCl_4$, have been identified by calorimetry and X-ray diffraction. The compounds, isostructural with each other, have unusual tetragonal

0108-7681/91/030337-08$03.00

structures when compared with other compounds of the same A_2BX_4 family. The structures at room temperature consist of layers of MCl_4^{2-} tetrahedral anions stacked perpendicular to the **c** direction and alternating with layers of $(CH_3)_4As^+$ tetrahedral cations. The average structure of this phase has space-group symmetry $I4_1/a$ ($Z = 8$). Data at 293 K: $[(CH_3)_4As]_2CoCl_4$, $M_r = 470{\cdot}6$, tetragonal, $P4_2/mbc$, $a = 17{\cdot}831$ (2), $c = 25{\cdot}20$ (1) Å, $V = 8011$ (4) Å^3, $Z = 16$, $D_m = 1{\cdot}54$ (2), $D_x = 1{\cdot}56$ g cm^{-3}, λ(Mo $K\alpha$) = 0·7107 Å, $\mu = 31{\cdot}17$ cm^{-1}, $F(000) = 3728$, $R = 0{\cdot}037$ for 1318 independent observed [$I > 3\sigma(I)$] reflections; $[(CH_3)_4As]_2ZnCl_4$, $M_r = 477{\cdot}3$, tetragonal, $P4_2/mbc$, $a = 17{\cdot}824$ (2), $c = 25{\cdot}209$ (3) Å, $V = 8008$ (2) Å^3, $Z = 16$, $D_x = 1{\cdot}58$ g cm^{-3}, λ(Cu $K\alpha$) = 1·54178 Å, $\mu = 103{\cdot}3$ cm^{-1}, $F(000) = 3776$, $R = 0{\cdot}096$ for 1821 independent observed [$I > 1{\cdot}5\sigma(I)$] reflections. In the low-temperature range of the intermediate phase, the diffraction pattern of $[(CH_3)_4As]_2CoCl_4$ shows satellite reflections which disappear before the next transition. It is unclear whether they are attributable to incommensurate modulation, twinning, or a combination of both effects.

1. Introduction

Compounds of the type $[(CH_3)_4N]_2MX_4$ [hereafter $(TMA)_2MX_4$], with M = first-row transition metal and X = Cl, Br, I, exhibit several phase transitions which may lead to modulated commensurate or incommensurate (IC) structures. All compounds have a common high-temperature structure of space group *Pmcn* (with $b \simeq a3^{1/2}$) and most of them can be placed in a common pressure–temperature diagram (Gesi, 1986). Furthermore, in general, the wavevector (**q**) of the commensurate or incommensurate structural modulation is parallel to the **c*** direction.

In constrast with this general behavior, some compounds, namely $(TMA)_2CuBr_4$, $(TMA)_2CdI_4$ and $(TMA)_2ZnI_4$, have been found to exhibit a sequence of transitions giving structural modulations with wavevector **q** parallel to the **b*** direction (Hasabe, Mashiyama & Tanisake, 1985; Kallel, Bats & Daoud, 1981; Werk, Chapuis & Zúñiga, 1990). These compounds also have a common *Pmcn* high-temperature structure and the space group of the modulated structure is $Pbc2_1$ ($\mathbf{q} = \frac{1}{2}\mathbf{b}^*$) or a subgroup.

The study of the dependence of the transition sequence on cation and anion sizes has recently been extended with a series of compounds based on larger quaternary organic cations. The transition sequence of $[(CH_3)_4P]_2CuCl_4$ (Pressprich, Bond, Willett & White, 1989) presents an incommensurate phase with **q** parallel to **c***, analogous to the general $(TMA)_2MX_4$ situation. On the other hand, the compound $[(CH_3)_4P]_2CuBr_4$ presents a sequence of phases with modulation parallel to **b*** (Madariaga, Alberdi & Zúñiga, 1990). In this paper, the structures and phase-transition sequences of two new compounds, based on the tetramethylarsonium (TMAs) cation, are presented.

2. Experimental

2.1. *Synthesis*

Bis(tetramethylarsonium) tetrachlorocobaltate(II) and -zincate(II) were obtained from an alcohol solution containing stoichiometric amounts of tetramethylarsonium chloride and the appropiate metal(II) chloride. The washed and dried precipitate was dissolved in acetonitrile and crystals were grown by slow evaporation. The compounds were analyzed for M^{2+} spectrophotometrically. Zn^{2+} and Co^{2+} were complexed with dithizone and analyzed using the 'mono-color' method (Marczenko, 1986): % found (% calculated), $(TMAs)_2CoCl_4$, 12·37 (12·52); $(TMAs)_2ZnCl_4$, 13·52 (13·70).

2.2. *Calorimetry*

Phase transitions were characterized on a Perkin–Elmer DSC7 using a scan rate of 5 K min^{-1}. Measurements on $(TMAs)_2CoCl_4$ between 303 and 573 K reveal thermal anomalies at 338 and 546 K with associated enthalpy changes of 2700 and 1300 J mol^{-1} respectively. Results for $(TMAs)_2ZnCl_4$ are the same within experimental uncertainties, showing anomalies at 336 and 549 K with associated enthalpy changes of 2700 and 1600 J mol^{-1} respectively. The three phases connected by these transitions will be referred to as III, II and I with increasing temperature. The thermal hysteresis and the peak shape of the III–II transition points towards a first-order type transition. The transition at 548 K is probably second order.

2.3. *Room-temperature X-ray structural analysis of* $(TMAs)_2CoCl_4$

For the resolution of the phase III structure of $(TMAs)_2CoCl_4$ at room temperature, a crystal with square-bipyramidal morphology and dimensions 0·02 × 0·02 × 0·04 cm was mounted on an automated four-circle diffractometer (CAD-4). The lattice constants given in the *Abstract* were calculated from the setting angles of 25 accurately centered reflections ($10 < \theta < 20°$), used in a tetragonally constrained refinement. Intensities of reflections out to $(\sin\theta/\lambda)_{max} = 0{\cdot}605$ Å^{-1} with indices in the ranges 0→21, 0→21 and 0→29 for h, k and l respectively were measured by a θ–2θ scan technique with intensity-dependent scan speeds varying between 4·12 and 0·5° min^{-1}. Three check reflections were

measured every hour. The backgrounds were evaluated by analyzing scan profiles (Schwarzenbach, 1977). The standard deviations of intensities were obtained from counting statistics.

The intensities were corrected for absorption by the Gaussian integration method; the transmission factor varied between 0·5608 and 0·4873; the R_{int} values from merging equivalent reflections were 0·033 and 0·044 with and without absorption corrections respectively. From a total of 8470 collected reflections, averaging of the data yielded 3571 independent reflections, of which 1318 had observed intensities according to the criterion $I > 3\sigma(I)$.

For the reduction of the data to $|F|$ moduli and refinement of the structure, the *XRAY*72 system of programs (Stewart, Kruger, Ammon, Dickinson & Hall, 1972; modified by D. Schwarzenbach) was used. Atomic scattering factors of neutral Co, Cl, As and C (Cromer & Mann, 1968); and anomalous-dispersion terms for Co, As and Cl (Cromer & Liberman, 1970) were used for the structure-factor calculations. The hydrogen atoms were not considered.

The structure was solved by direct methods with *MULTAN*84 (Main *et al.*, 1984). Based on the intensity statistics, the solution was only searched in the centrosymmetric space group. The structure was refined by full-matrix least squares. The function minimized was $\sum(w\Delta F)^2$ with $w = 1/\sigma^2(F)$. All atoms were refined with anisotropic thermal displacements. In the last steps of the refinement, a total of 142 parameters were varied, including an extinction parameter; maximum final parameter shift/e.s.d. was 1·5. The residual based on F values is $wR = 0{\cdot}049$ with $S = 3{\cdot}38$. A final difference Fourier synthesis showed high peaks of up to 1·9 e Å^{-3} around the As atoms. The atomic parameters are reported in Table 1.*

Table 1. *Atomic parameters for* $(TMAs)_2CoCl_4$ *and* $(TMAs)_2ZnCl_4$ *at* 293 K

Equivalent isotropic U is defined as one third of the trace of the orthogonalized U_{ij} tensor.

	x	y	z	U_{eq} (Å^2)
(*a*) $(TMAs)_2CoCl_4$				
Co(1)	0	0	0·25	0·044 (2)
Co(2)	0·5	0	0·25	0·046 (2)
Co(3)	0·22619 (8)	0·2472 (1)	0·5	0·0599 (6)
Cl(1)	0·1032 (1)	−0·0116 (2)	0·1988 (2)	0·080 (2)
Cl(2)	0·3957 (1)	0·0012 (1)	0·3006 (2)	0·080 (2)
Cl(31)	0·1279 (2)	0·3280 (2)	0·5	0·071 (1)
Cl(32)	0·1794 (2)	0·1293 (2)	0·5	0·117 (2)
Cl(33)	0·2930 (2)	0·2666 (2)	0·4262 (1)	0·151 (2)
As(1)	0·29321 (6)	0·00380 (5)	0·12517 (7)	0·0582 (6)
As(2)	0·20573 (6)	−0·00727 (5)	0·37423 (7)	0·0584 (6)
C(11)	0·2083 (5)	0·0049 (4)	0·0772 (7)	0·068 (4)
C(12)	0·3831 (5)	0·0254 (6)	0·0867 (6)	0·097 (6)
C(13)	0·2815 (5)	0·0776 (5)	0·1803 (5)	0·072 (4)
C(14)	0·2976 (5)	−0·0939 (5)	0·1590 (5)	0·088 (5)
C(21)	0·2113 (5)	0·0888 (4)	0·3403 (5)	0·088 (5)
C(22)	0·1122 (5)	−0·0173 (5)	0·4116 (6)	0·079 (5)
C(23)	0·2852 (4)	−0·0199 (5)	0·4229 (6)	0·074 (5)
C(24)	0·2094 (5)	−0·0837 (5)	0·3196 (5)	0·083 (4)
(*b*) $(TMAs)_2ZnCl_4$				
Zn(1)	0	0	0·25	0·041 (2)
Zn(2)	0·5	0	0·25	0·040 (1)
Zn(3)	0·2261 (1)	0·2474 (1)	0·5	0·054 (1)
Cl(1)	0·1032 (2)	−0·0116 (2)	0·1990 (1)	0·077 (1)
Cl(2)	0·3956 (2)	0·0011 (2)	0·3006 (1)	0·076 (1)
Cl(31)	0·1281 (2)	0·3280 (2)	0·5	0·065 (2)
Cl(32)	0·1794 (3)	0·1296 (2)	0·5	0·107 (2)
Cl(33)	0·2919 (3)	0·2662 (2)	0·4254 (2)	0·143 (2)
As(1)	0·2932 (1)	0·0036 (1)	0·1250 (1)	0·055 (1)
As(2)	0·2058 (1)	−0·0073 (1)	0·3740 (1)	0·053 (1)
C(11)	0·2104 (6)	0·0048 (5)	0·0783 (4)	0·061 (4)
C(12)	0·3848 (6)	0·0240 (7)	0·0885 (4)	0·111 (7)
C(13)	0·2838 (6)	0·0775 (6)	0·1786 (4)	0·068 (4)
C(14)	0·2995 (6)	−0·0913 (7)	0·1575 (5)	0·089 (6)
C(21)	0·2129 (7)	0·0861 (7)	0·3422 (5)	0·093 (6)
C(22)	0·1128 (6)	−0·0174 (6)	−0·4112 (5)	0·089 (6)
C(23)	0·2860 (6)	−0·0176 (7)	0·4224 (5)	0·079 (5)
C(24)	0·2100 (6)	−0·0836 (6)	0·3218 (4)	0·074 (5)

2.4. *Room-temperature X-ray structural analysis of* $(TMAs)_2ZnCl_4$

For the analogous resolution of the phase III structure of $(TMAs)_2ZnCl_4$ at room temperature, a crystal with a brick-like morphology having truncated edges and dimensions 0·02 × 0·03 × 0·05 cm was mounted on a Nicolet *R*3*m* diffractometer with Cu $K\alpha$ radiation and a graphite monochromator (Campana, Shepard & Litchman, 1981). The lattice constants given in the *Abstract* were calculated from 25 reflections ($0{\cdot}38 < \sin\theta/\lambda < 0{\cdot}46$ Å^{-1}) in a tetragonally constrained refinement. Intensities of reflections out to $(\sin\theta/\lambda)_{max} = 0{\cdot}525$ Å^{-1} with indices in the range $0 \rightarrow 18$, $-12 \rightarrow 18$ and $0 \rightarrow 26$ for h, k, and l respectively were measured by ω–2θ scans with scan speeds varying between 29·30 and 3·91° min^{-1}. Two check reflections were measured every 100 reflections. Variations were within counting statistics. E.s.d.'s of intensities were obtained from counting statistics.

Data reduction and refinement were completed with Nicolet *SHELXTL* programs (Sheldrick, 1986). Intensities were corrected for absorption by the Gaussian integration method. Transmission varied between 0·05 and 0·24. From a total of 6697 collected reflections (some redundant), averaging of data yielded 2332 independent reflections, of which 1821 were observed with $I > 1{\cdot}5\sigma(I)$. For equivalent reflections $R_{int} = 0{\cdot}100$ after correcting for absorption. Initially, the space group $P4_2/mbc$ was tested. The direct methods program *SOLV* (Sheldrick, 1986) and subsequent blocked-cascade least-squares refinement resolved all non-hydrogen atoms. Further refinements included anisotropic thermal parameters for non-hydrogen atoms with isotropic thermal

* Lists of structure factors, anisotropic thermal parameters for both compounds and H-atom parameters for $(TMAs)_2ZnCl_4$ have been deposited with the British Library Document Supply Centre as Supplementary Publication No. SUP 53714 (28 pp.). Copies may be obtained through The Technical Editor, International Union of Crystallography, 5 Abbey Square, Chester CH1 2HU, England.

parameters for hydrogen atoms constrained to values approximately 20% larger than those of their corresponding carbon atoms. Hydrogen atoms were further constrained to idealized methyl group geometries with C—H = 0·96 Å. The function minimized was $\Sigma(w\Delta F)^2$ with $w = [\sigma^2(F_o) + g(F_o)]$, $g = 0{\cdot}005$ and the number of parameters = 142 (including an extinction parameter). In this centrosymetric refinement, $R = 0{\cdot}096$, $wR = 0{\cdot}127$ and $S = 1{\cdot}37$ for observed reflections. For all unique reflections, $R = 0{\cdot}109$ and $wR = 0{\cdot}136$. The largest residual on the final difference map was 1·4 e Å^{-3} near As(2). Final maximum and mean parameter shifts/e.s.d. were −0·014 and 0·003 respectively. Refinement in the non-centrosymetric space group $P4_2bc$ gave no significant atomic shifts and led to worse atomic e.s.d.'s. Atomic parameters are reported in Table 1.

2.5. *Temperature-dependent X-ray studies of* $(TMAs)_2CoCl_4$

Preliminary X-ray diffraction experiments were performed using a Buerger precession camera with an Enraf–Nonius high-temperature device. Single-crystal diffractograms were obtained at room temperature, 353, 393 and 423 K. A thermal stability of ± 3 K and a total uncertainty of ± 5 K were estimated. All diffractograms were taken using the same type of film and with controlled exposure times.

At room temperature, the precession diffractograms show tetragonal symmetry and the observed systematic absences are compatible with space groups $P4_2/mbc$ or $P4_2bc$. The former was later confirmed from refinement of the structure. An important characteristic of the diffraction patterns is that, in general, all reflections (h,k,l) with $h + k$, $h + l$, and $k + l$ all odd are very weak, so the structure has the pseudosymmetry of an *F*-centered lattice.

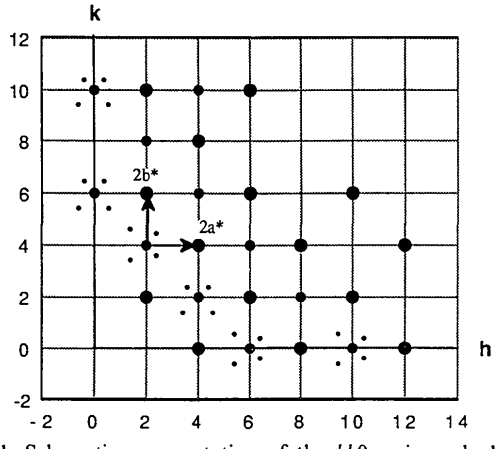

Fig. 1. Schematic representation of the *hk*0 reciprocal plane as observed by precession diagrams at 353 K. Commensurate spots are represented by large ($h + k = 4n$) and medium circles, and satellites by small circles.

In the diffraction patterns obtained at 353 K new weak satellite reflections, clearly incommensurate with the room-temperature tetragonal subcell, appear at the reciprocal lattice points $(h \pm \delta, k \pm \delta, l)$, with δ close to 0·41 or 0·59. Fig. 1 shows a diagram of the $(hk0)$ layer. As is usual for incommensurate structures, all the satellite reflections can be indexed with two additional integers m_1 and m_2, related to two vectors:

$$\mathbf{q}_1 = (\tfrac{1}{2} + \delta)(\mathbf{a}^* + \mathbf{b}^*)$$
$$\mathbf{q}_2 = (\tfrac{1}{2} + \delta)(\mathbf{a}^* - \mathbf{b}^*)$$

with $\mathbf{a}^*$ and $\mathbf{b}^*$ referred to the basic reciprocal lattice of phase III. A rough value of the δ parameter measured on the photographs at 353 K is $\delta = 0{\cdot}09$. According to the above scheme for indexing the satellites, each main reflection has associated with it four possible first-order satellite reflections (h,k,l,m_1,m_2) *with* m_1 and m_2 equal to ± 1, but only two of them are observed. In addition, the general rule of systematic absences (h,k,l,m_1,m_2) $l = 2n + 1$ is strictly observed for the satellite reflections. For the main reflections, the diffraction pattern has the same symmetry as that at room temperature. However, those main reflections corresponding to systematic absences of the *F*-centered lattice are clearly weaker than at 293 K, and the reflections $(hk0)$ with $h + k \neq 4n$ show a tendency to vanish, which indicates the appearance of a *d*-diagonal glide plane.

At 393 K the satellite reflections are still visible but clearly with diminished intensity and the diffraction pattern has the same characteristics as before. For main reflections, the new systematic absences of the *F*-centered lattice are definitively confirmed from precession photographs at 423 K. Satellite reflections are weak or unobserved at this temperature (see below). Therefore, at this temperature the structure corresponds to an $F4_1/d$ space group if the room-temperature orientation of basis vectors is retained and any residual satellite reflections are ignored. A cell transformation:

$$\mathbf{a}' = \tfrac{1}{2}(\mathbf{a} + \mathbf{b})$$
$$\mathbf{b}' = \tfrac{1}{2}(\mathbf{a} - \mathbf{b})$$

gives the standard $I4_1/a$ space group with new lattice constants $a = 12{\cdot}61$ and $c = 25{\cdot}44$ Å, and $Z = 8$.

3. Discussion

The phase behavior and room-temperature structures of $(TMAs)_2MCl_4$ (M = Co, Zn) have been determined. Both salts show a phase sequence:

III	→	II	→	I
Tetragonal		Tetragonal		Unknown
$P4_2/mbc$		$I4_1/a$		

Table 2. *Selected interatomic distances* (Å) *and angles* (°) *for* $(TMAs)_2CoCl_4$ *and* $(TMAs)_2ZnCl_4$, *with e.s.d.'s in parentheses*

	Uncorrected	Corrected		Uncorrected
(*a*) $(TMAs)_2CoCl_4$				
Co(1)—Cl(1)	2·256 (3)	2·281	Cl(31)—Co(3)—Cl(32)	107·7 (1)
Co(2)—Cl(2)	2·255 (3)	2·277	Cl(31)—Co(3)—Cl(33)	108·2 (1)
Co(3)—Cl(31)	2·269 (3)	2·301	Cl(32)—Co(3)—Cl(33)	109·9 (1)
Co(3)—Cl(32)	2·261 (4)	2·307	Cl(33)—Co(3)—Cl(33)^{vii}	112·5 (1)
Co(3)—Cl(33)	2·235 (3)	2·282		
			C(11)—As(1)—C(12)	109·7 (6)
As(1)—C(11)	1·93 (1)	1·96	C(11)—As(1)—C(13)	110·9 (4)
As(1)—C(12)	1·91 (2)	1·94	C(11)—As(1)—C(14)	108·3 (4)
As(1)—C(13)	1·92 (1)	1·94	C(12)—As(1)—C(13)	108·5 (4)
As(1)—C(14)	1·941 (9)	1·97	C(12)—As(1)—C(14)	111·6 (4)
As(2)—C(21)	1·917 (9)	1·94	C(13)—As(1)—C(14)	107·5 (4)
As(2)—C(22)	1·92 (1)	1·94		
As(2)—C(23)	1·88 (1)	1·91	C(21)—As(2)—C(22)	110·2 (4)
As(2)—C(24)	1·93 (1)	1·96	C(21)—As(2)—C(23)	110·9 (4)
			C(21)—As(2)—C(24)	108·0 (4)
Cl(1)—Co(1)—Cl(1)^{i}	109·0 (1)		C(22)—As(2)—C(23)	108·7 (5)
Cl(1)—Co(1)—Cl(1)^{ii}	110·2 (1)		C(22)—As(2)—C(24)	108·1 (4)
Cl(1)—Co(1)—Cl(1)^{iii}	109·0 (1)		C(23)—As(2)—C(24)	110·6 (4)
Cl(2)—Co(2)—Cl(2)^{iv}	107·6 (1)			
Cl(2)—Co(2)—Cl(2)^{v}	111·1 (1)			
Cl(2)—Co(2)—Cl(2)^{vi}	109·6 (1)			
(*b*) $(TMAs)_2ZnCl_4$				
Zn(1)—Cl(1)	2·253 (3)	2·276	Cl(31)—Zn(3)—Cl(32)	107·8 (2)
Zn(2)—Cl(2)	2·256 (3)	2·278	Cl(31)—Zn(3)—Cl(33)	108·0 (1)
Zn(3)—Cl(31)	2·262 (4)	2·293	Cl(32)—Zn(3)—Cl(33)	109·4 (1)
Zn(3)—Cl(32)	2·259 (5)	2·302	Cl(33)—Zn(3)—Cl(33)^{vii}	114·1 (3)
Zn(3)—Cl(33)	2·241 (5)	2·283		
			C(11)—As(1)—C(12)	111·5 (5)
As(1)—C(11)	1·888 (11)	1·90	C(11)—As(1)—C(13)	111·5 (4)
As(1)—C(12)	1·909 (10)	1·93	C(11)—As(1)—C(14)	109·2 (5)
As(1)—C(13)	1·894 (10)	1·90	C(12)—As(1)—C(13)	106·7 (5)
As(1)—C(14)	1·884 (12)	1·91	C(12)—As(1)—C(14)	109·3 (5)
As(2)—C(21)	1·853 (13)	1·88	C(13)—As(1)—C(14)	108·6 (5)
As(2)—C(22)	1·913 (12)	1·93		
As(2)—C(23)	1·889 (12)	1·91	C(21)—As(2)—C(22)	110·9 (5)
As(2)—C(24)	1·893 (11)	1·91	C(21)—As(2)—C(23)	108·3 (5)
			C(21)—As(2)—C(24)	110·0 (5)
Cl(1)—Zn(1)—Cl(1)^{i}	109·0 (1)		C(22)—As(2)—C(23)	109·3 (5)
Cl(1)—Zn(1)—Cl(1)^{ii}	110·5 (2)		C(22)—As(2)—C(24)	108·0 (5)
Cl(1)—Zn(1)—Cl(1)^{iii}	109·0 (1)			
			C(23)—As(2)—C(24)	110·4 (5)
Cl(2)—Zn(2)—Cl(2)^{iv}	111·1 (1)			
Cl(2)—Zn(2)—Cl(2)^{v}	107·8 (2)			
Cl(2)—Zn(2)—Cl(2)^{vi}	109·5 (2)			

Symmetry operation: (i) $y, -x, \frac{1}{2}-z$; (ii) $-x, -y, z$; (iii) $-y, x, \frac{1}{2}-z$; (iv) $1-x, -y, z$; (v) $\frac{1}{2}-y, \frac{1}{2}-x, \frac{1}{2}-z$; (vi) $\frac{1}{2}+y, -\frac{1}{2}+x, \frac{1}{2}-z$; (vii) $x, y, 1-z$.

The structures are in fact somewhat surprising since they are the first reported compounds of the A_2BX_4 family which do not possess either the prototype β-K_2SO_4 *Pmcn* structure found in $[(CH_3)_4N]_2MX_4$ (M = Co, Zn, Cu and X = Cl, Br) (Wiesner, Srivastava, Kennard, Divaira & Lingafelter, 1967; Trouelan, Lefebvre & Derollez, 1984) or a slightly perturbed subgroup variation.

Since the phase transitions and structures of $(TMAs)_2ZnCl_4$ and $(TMAs)_2CoCl_4$ are identical within experimental uncertainties, further discussion will center on $(TMAs)_2CoCl_4$ with the understanding that identical arguments apply to $(TMAs)_2ZnCl_4$.

The bond lengths and angles for $(TMAs)_2CoCl_4$ are given in Table 2. The analysis of the thermal displacements in terms of *TLS* tensors (Schomaker & Trueblood, 1968), shows that all of the $[CoCl_4]^{2-}$ and $[Me_4As]^{4+}$ tetrahedra can be described quite accurately as rigid-body ions. The tetrahedron around the Co(3) atom has the largest thermal displacements, which involve rotations of 8° and translations of 0·2 Å. The room-temperature structures can be described as alternating layers of tetrahedral MCl_4^{2-} (M = Co, Zn) and $TMAs^+$ ions, stacked along the c direction. A stereoview of the structure of $(TMAs)_2CoCl_4$ phase III is shown in Fig. 2. All the M atoms are located on special positions. Atoms $M(1)$ and $M(2)$ lie on fourfold positions of 4 and 222 symmetry respectively, forming layers at $z = \frac{1}{4}$ and $\frac{3}{4}$, while $M(3)$ atoms, in eightfold positions, are distributed on mirror planes at $z = 0$ and $\frac{1}{2}$. The tetramethylarsonium ions are intercalated into general positions between adjacent MCl_4-tetrahedra layers, and form layers at z = 0·125, 0·375, 0·625 and 0·875. Therefore, the different structural layers are equally spaced by 0·125 along the c axis. Two sections through the structure projected down **c** are shown in Figs. 3(*a*) and 3(*b*).

The results described in §2.5 are not sufficient to prove that an incommensurate phase exists in the low-temperature region of phase II. The satellite reflections appear and disappear between two transitions detected by calorimetry at 338 and 546 K, which could indicate the existence of an additional transition. The same experiments performed with different crystals gave similar results, but with the appearance and disappearance of satellite reflections taking place at different temperatures. For instance, in one case, whereas main reflections (600) and (10,0,0) disappeared at 423 K, their neighboring satellite reflections could still be observed.

These results could also be interpreted if a twinned crystal is formed on heating above the III–II transition temperature. Such twins should be related to a high-temperature phase with cubic symmetry and lattice parameter a = 25·2 Å. Note that directions [100] and [001] in the I-centered cell becomes equivalent in the cubic phase and so twinned crystals with parallel [100] and [001] directions could be formed.

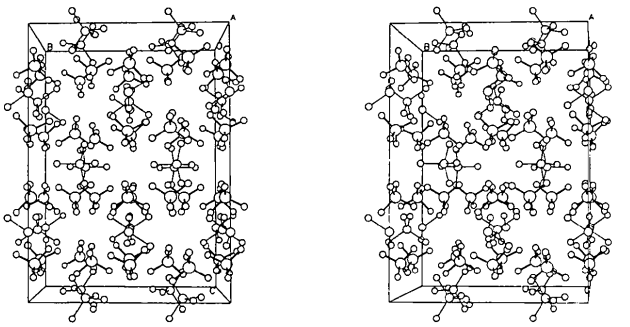

Fig. 2. Stereoscopic view of the structure of $(TMAs)_2CoCl_4$ at room temperature. The thick bonds correspond to the TMAs tetrahedra.

Supposing that the transition II–I is of second-order type, the only possible point group with cubic symmetry is *m3m*. This means that there may be six twin domains with ferroelastic character in phase II. Mechanical stress might induce a change in the relative percentage of the twin domains during the annealing process.

Concerning phase II, we can conclude from the experimental results that the structure is commensurate, with space group $I4_1/a$ at temperatures well above the first transition temperature. This space group can be anticipated from the room-temperature diffractograms, which show only minor violations of the extinctions for an *F*-centered lattice. Just above the III–II transition at 340 K, the structure appears to be incommensurate. However, we cannot confirm if the basic lattice corresponds to that of the room-temperature structure or to the *I*-centered one. The satellite reflections above the first transition coexist with main reflections that violate the extinctions of the *F*-centered lattice. However, this latter class of reflections clearly shows a tendency to disappear as the temperature is increased, and therefore their presence above 340 K can be interpreted as due to the coexistence of phases II and III. In any case, we can say that phase II has an average structure with an $I4_1/a$ space group and the lattice constants reported in §2. Less can be said about the structure of phase I. This phase does appear after a second-order phase transition and so the changes are expected to be small.

Table 3. *Atomic coordinates of the* Co *and* As *atoms in phase* III *referred to the I-centered cell and hypothetical coordinates of the same atoms in the high-temperature phase* II

	Phase III			Phase II		
	x	*y*	*z*	*x*	*y*	*z*
Co(1)	0	0	0·25	0	0	0·25
Co(2)	0·50	0·5	0·25	0·5	0·5	0·25
Co(3)	0·4734	−0·021	0·5	0·5	0	0·5
As(1)	0·2970	0·2892	0·1252	0·292	0·244	0·125
As(2)	0·1984	0·2130	0·3742	0·244	0·208	0·375

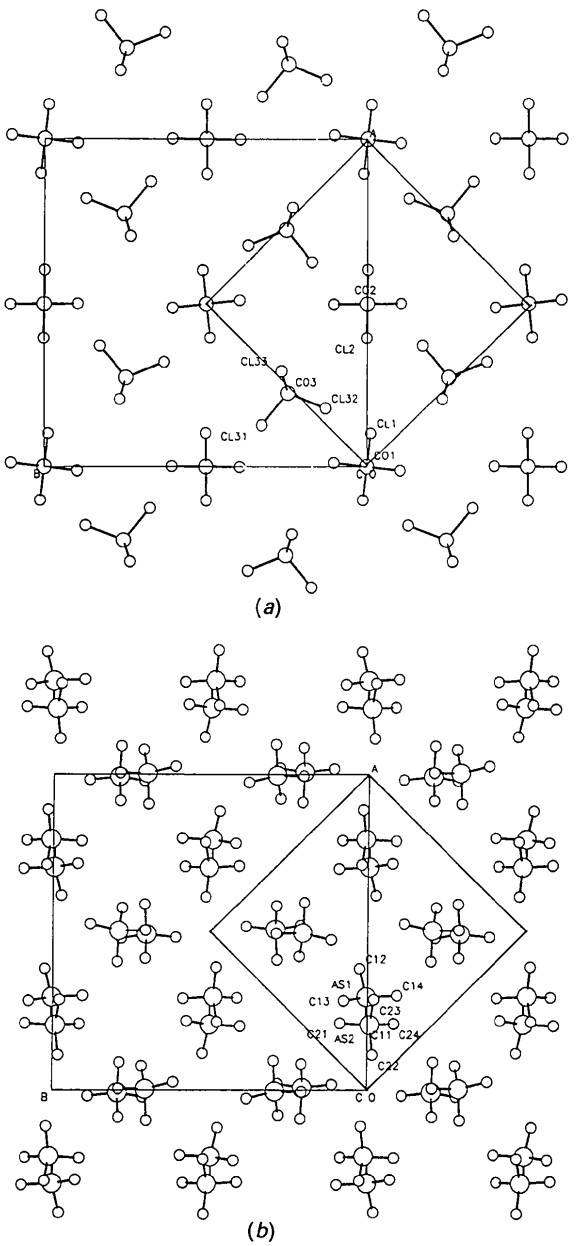

Fig. 3. Projections along the *c* axis of (*a*) two consecutive layers of $CoCl_4^{2-}$ tetrahedra at $z = 0$, 0·25 and (*b*) two consecutive layers of AsO_4 tetrahedra at $z = 0{\cdot}125$, 0·375. The *I*-centered high-temperature cell is outlined on the same projections.

The pseudoextinction of the *F*-centered lattice observed at room temperature can be understood by the arrangement of the Co and As atoms, which form a structure close to that of an *F*-centered lattice. Then Co(1) and Co(2) become symmetry equivalent, as do As(1) and As(2). Co(3) must be displaced from the (0·2262, 0·2472, 0·5) coordinates to $(\frac{1}{4},\frac{1}{4},\frac{1}{2})$, which corresponds to an atomic displacement of 0·427 Å. As(1) and As(2) become related by a center of inversion $\{I|\frac{1}{2},0,\frac{1}{2}\}$ requiring net displacements of As(1) and As(2) of 0·069 and 0·131 Å respectively. Figs. 3(*a*) and 3(*b*) show a projection along the *c* axis of two consecutive layers of $CoCl_4$ tetrahedra (*a*), and two layers of TMAs tetrahedra (*b*) with the primitive and high-temperature *I*-centered cell outlined.

This structural model may be adapted to phase II. The coordinates of the Co and As atoms in a hypothetical $I4_1/a$ structure are summarized in Table 3. The coordinates correspond to placing the origin at the site of 4 symmetry. In this hypothetical model Co(1), Co(2) and Co(3) are symmetry equivalent, having the coordinates of the special set of positions

with 2 symmetry. As(1) and As(2) are also symmetry equivalent, occupying a general set of positions. The element relating them, $\{C_{4z}^{-}|0,\frac{1}{2},\frac{1}{4}\}$, requires a net displacement of As(1) and As(2) of 1·15 Å. An alternative hypothetical $I4_1/a$ structure places the Co atoms, no longer all equivalent, at the two special sets of positions having 4 symmetry. This alternative again relates the As atoms as mentioned above, by a $\{C_{4z}^{-}|0,\frac{1}{2},\frac{1}{4}\}$ element and with a 1·15 Å net displacement from their room-temperature positions.

As mentioned above, $(TMAs)_2CoCl_4$ is the first reported compound of the $(TMPc)_2BX_4$ type (Pc = N, P, As, Sb), which exhibits tetragonal symmetry and which does not retain a group–subgroup relation with the prototype *Pmcn* space group. However, the question arises as to whether a relationship between both structures can be found. To this end, we have chosen $(TMA)_2CoCl_4$, which exhibits an extensive phase-transition sequence, with several structural distortions of the high-temperature *Pmcn* symmetry (Fjaer, 1985). The structural comparison should be made between the high-temperature phases of both compounds but, in the absence of exact coordinates for phase I of $(TMAs)_2CoCl_4$, we will compare the structures having symmetries *Pmcn* [$(TMA)_2CoCl_4$] and $P4_2/mbc$ [$(TMAs)_2CoCl_4$]. A relationship between the cell parameters is given by $\mathbf{a}_t \simeq \mathbf{a}_o + \mathbf{b}_o$ and $\mathbf{c}_t \simeq 2\mathbf{c}_o$ where the subscripts refer to the tetragonal (t) and orthorhombic (o) phases. Note that the above relation is given between vectors and that the transformation from the orthorhombic to the tetragonal cell includes an angular distortion between the a_t and b_t axes. Now, if we compare both structures with their c axes parallel, it is easy to see that the Co layers of $(TMAs)_2CoCl_4$ are also present in the $(TMA)_2CoCl_4$ compound. This result is shown in Fig. 4 where a schematic stacking of layers in both compounds is drawn. The most important difference is that the single-layer arrangement of the organic ions in the tetragonal structure corresponds to a thick layer of tetramethylammonium ions in the orthorhombic structure. Nevertheless, alternating stacking with similar interlayer spacing is evident in both structures. The structural similarities can be extended to the positions of the Co atoms on the layers, which can be seen in Fig. 5. In this figure, the Co atoms at $0{\cdot}25c_o$ and $0{\cdot}75c_o$ in the $(TMA)_2CoCl_4$ structure are represented over four orthorhombic cells, and in the same figure the distorted tetragonal cell is outlined. Note that, neglecting the angular distortion, the positions of these atoms in the tetragonal cell are in agreement with those of Fig. 2.

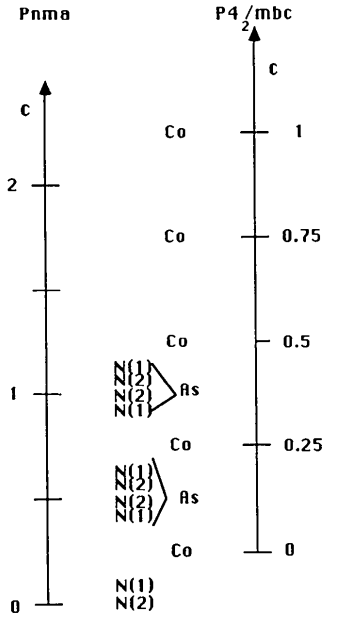

Fig. 4. Schematic representation of the distribution of layers of tetrahedra along the c axis in the structures of $(TMA)_2CoCl_4$ and $(TMAs)_2CoCl_4$.

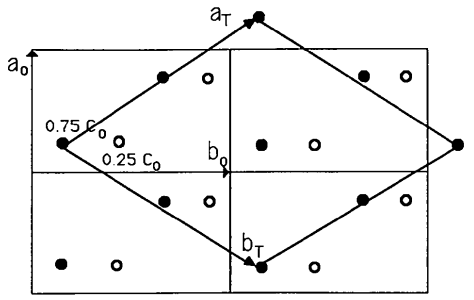

Fig. 5. Schematic representation of the projection along the **c** direction of the Co atoms in the orthorhombic structure of $(TMA)_2CoCl_4$. The axes labeled a_t and b_t define a distorted cell close to the tetragonal cell of $(TMAs)_2CoCl_4$.

This work was supported by the Spanish DGICYT, project No. PB87-0744, and by ACS-PRF grant No. 20215-AC3-C. We wish to thank Professor K. Emerson of Montana State University for introducing the two research groups.

References

CAMPANA, C. F., SHEPARD, D. F. & LITCHMAN, W. N. (1981). *Inorg. Chem.* **20**, 4039–4044.

CROMER, D. T. & LIBERMAN, D. (1970). *J. Chem. Phys.* **53**, 1891–1898.

CROMER, D. T. & MANN, J. B. (1968). *Acta Cryst.* A**24**, 321–324.

FJAER, E. (1985). *Acta Cryst.* B**41**, 330–336.

GEST, K. (1986). *Ferroelectrics*, **66**, 269–286.

HASABE, K., MASHIYAMA, H. & TANISAKI, S. (1985). *Jpn. J. Appl. Phys.* **24**, 758–760.

KALLEL, A., BATS, J. W. & DAOUD, A. (1981). *Acta Cryst.* B**37**, 676–677.

MADARIAGA, G., ALBERDI, M. M. & ZÚÑIGA, F. J. (1990). *Acta Cryst.* C**46**, 2363–2366.
MAIN, P., FISKE, S. J., HULL, S. E., LESSINGER, L., GERMAIN, G., DECLERCQ, J.-P. & WOOLFSON, M. M. (1984). *MULTAN*11/84. *A System of Computer Programs for the Automatic Solution of Crystal Structures from X-ray Diffraction Data.* Univs. of York, England, and Louvain, Belgium.
MARCZENKO, Z. (1986). In *Separation and Spectrophotometric Determination of Elements.* New York: Halsted Press.
PRESSPRICH, M. R., BOND, M. R., WILLETT, R. D. & WHITE, M. A. (1989). *Phys. Rev.* **39**, 3453–3456.
RAGER, H. & WEISS, A. (1974). *Z. Phys. Chem.* **93**, 299–312.
SCHOMAKER, V. & TRUEBLOOD, K. N. (1968). *Acta Cryst.* B**24**, 63–76.
SCHWARZENBACH, D. (1977). 4th Eur. Crystallogr. Meet., Oxford, Abstract PI 20.
SHELDRICK, G. M. (1986). *SHELXTL.* Version 5.1. Nicolet Analytical Instruments, Madison, Wisconsin, USA.
STEWART, J. M., KRUGER, G. J., AMMON, H. L., DICKINSON, C. W. & HALL, S. R. (1972). The *XRAY*72 system – version of June 1972. Tech. Rep. TR-192. Computer Science Center, Univ. of Maryland, College Park, Maryland, USA.
TROUELAN, P., LEFEBVRE, J. & DEROLLEZ, P. (1984). *Acta Cryst.* C**40**, 386–389.
WERK, M. L., CHAPUIS, G. & ZÚÑIGA, F. J. (1990). *Acta Cryst.* B**46**, 187–192.
WIESNER, J. R., SRIVASTAVA, R., KENNARD, C. H. L., DIVAIRA, M. & LINGAFELTER, E. C. (1967). *Acta Cryst.* **23**, 565–574.

Acta Cryst. (1991). B**47**, 344–355

Correlation of Electron Density and Spin-Exchange Interaction in Dimeric Copper(II) Formates, Acetates and Silanecarboxylates

BY MICHINARI YAMANAKA, HIDEHIRO UEKUSA, SHIGERU OHBA, YOSHIHIKO SAITO* AND SUEHIRO IWATA

Department of Chemistry, Faculty of Science and Technology, Keio University, Hiyoshi, Kohoku-ku, Yokohama 223, *Japan*

MICHINOBU KATO

Aichi Prefectural University, Mizuho-ku, Nagoya 467, *Japan*

TADASHI TOKII AND YONEICHIRO MUTO

Department of Chemistry, Faculty of Science and Engineering, Saga University, Saga 840, *Japan*

AND OMAR W. STEWARD

Department of Chemistry, Duquesne University, Pittsburgh, PA 15282, *USA*

(*Received* 10 *August* 1990; *accepted* 2 *November* 1990)

Abstract

The structures of six dimeric copper(II) formates and acetates with picoline as an axial ligand, (I)–(VI), have been determined at room temperature and electron density distributions in lithium acetate dihydrate, (VII), and copper(II) formate diurea dihydrate, (VIII), have been studied at 120 K. Mo $K\alpha$ radiation was used throughout (λ = 0·71073 Å): tetrakis(μ-formato-O,O')-bis(α-picoline)dicopper(II), $[Cu(HCOO)_2\alpha\text{-pic}]_2$, (I), M_r = 493·42, triclinic, $P\bar{1}$, a = 7·310 (1), b = 10·493 (2), c = 7·291 (1) Å, α = 91·35 (2), β = 113·93 (1), γ = 109·24 (2)°, V = 474·5 (1) Å^3, Z = 1, D_x = 1·73 Mg m^{-3}, μ = 2·29 mm^{-1}, $F(000)$ = 250, R = 0·029 for 1675 reflections; $[Cu(HCOO)_2\beta\text{-pic}]_2$, (II), triclinic, $P\bar{1}$, a = 10·922 (3), b = 13·123 (2), c = 7·208 (2) Å, α = 98·64 (2), β = 109·11 (2), γ = 83·39 (2)°, V = 962·6 (3) Å^3, Z = 2, D_x = 1·70 Mg m^{-3}, μ = 2·26 mm^{-1}, $F(000)$ = 500, R = 0·032 for 2629 reflections; $[Cu(HCOO)_2\gamma\text{-pic}]_2$, (III), monoclinic, $P2_1/c$, a = 10·695 (2), b = 11·373 (2), c = 7·755 (1) Å, β = 90·13 (2)°, V = 942·7 (3) Å^3, Z = 2, D_x = 1·74 Mg m^{-3}, μ = 2·31 mm^{-1}, $F(000)$ = 500, R = 0·027 for 1474 reflections; tetrakis(μ-acetato-O,O')-bis(α-picoline)dicopper(II), $[Cu(CH_3COO)_2\alpha\text{-pic}]_2$, (IV), M_r = 549·53, monoclinic, $P2_1/c$, a = 7·697 (1), b = 20·021 (3), c = 8·226 (1) Å, β = 116·0 (1)°, V = 1139·4 (3) Å^3, Z = 2, D_x = 1·60 Mg m^{-3}, μ = 1·92 mm^{-1}, $F(000)$ = 564, R = 0·051 for 1691 reflections; $[Cu(CH_3COO)_2\beta\text{-pic}]_2$, (V), triclinic, $P\bar{1}$, a = 8·315 (1), b = 20·242 (2), c = 7·789 (1) Å, α = 93·21 (1), β = 117·36 (1), γ = 92·74 (1)°, V = 1158·5 (2) Å^3, Z = 2, D_x = 1·58 Mg m^{-3}, μ = 1·89 mm^{-1}, $F(000)$ = 564, R = 0·063 for 3041 reflections; $[Cu(CH_3COO)_2\gamma\text{-pic}]_2$, (VI), monoclinic, $P2_1/c$, a = 10·499 (1), b = 13·031 (2), c = 8·880 (1) Å, β = 102·16 (1)°, V = 1187·6 (2) Å^3, Z = 2, D_x = 1·55 Mg m^{-3}, μ =

* To whom correspondence should be addressed.

0108-7681/91/030344-12$03.00